

Behavior of H₂O molecules in the channels of natrolite and scolecite: A Raman and IR spectroscopic investigation of hydrous microporous silicates

B.A. KOLESOV¹ AND C.A. GEIGER^{2,*}

¹Institute of Inorganic Chemistry, Russian Academy of Science, Lavrentiev prosp. 3, Novosibirsk 630090, Russia
²Institut für Geowissenschaften, Universität Kiel, Abteilung Mineralogie, Olshausenstr. 40, D-24098 Kiel, Germany

ABSTRACT

Single-crystal polarized Raman spectra (80 to 4000 cm⁻¹ at 4 ≤ *T* ≤ 700 K) and powder IR spectra (1500 to 4000 cm⁻¹ at 50 < *T* < 300 K) were measured for two microporous zeolites natrolite, Na₁₆[Al₁₆Si₂₄O₈₀]·16H₂O, and scolecite, Ca₈[Al₁₆Si₂₄O₈₀]·24H₂O to determine the behavior of H₂O molecules in the channels. Both IR and Raman spectra show intense O-H stretching and H₂O bending modes derived from the hydrogen-bonded H₂O molecule(s) in the channels. Using published crystal structural data for natrolite and scolecite, and a consideration of Raman mode intensities that are sensitive to the H₂O orientation in the framework channels, the internal stretching and bending modes could be assigned. The Raman spectra also show lower energy lattice modes and, in addition, second-order scattering in the wavenumber range where O-H stretching vibrations occur. The stretching vibrations of H₂O molecules of natrolite and scolecite are located between 3200 and 3700 cm⁻¹ and bending vibrations occur around 1650 cm⁻¹. In the case of natrolite, two intense O-H stretching modes can be observed and also several weaker combination modes. The latter was used to derive a low energy external H₂O translational vibration, T(H₂O), which is also observed directly in single-crystal Raman spectra. In addition, two H₂O librational modes are located at about 440 and 500 cm⁻¹. For scolecite, six O-H stretching modes are observed in the Raman spectra recorded at 4 K, but only five are found at room temperature in the IR or Raman. The single-crystal Raman spectra also show several second-order combination modes consisting of external and internal H₂O vibrations. They permit the wavenumber of several T(H₂O) modes at low wavenumbers to be determined. These combination bands are analyzed based on their temperature behavior between 0 and 300 K. It is shown that the wavenumber of the H₂O bending modes decreases with an increase of the H-O-H angle of the H₂O molecule in natrolite and scolecite. The dehydration behavior of H₂O in natrolite and scolecite was investigated by Raman measurements of the intensities of the O-H stretching modes at temperatures from 300 K to 570 K and 720 K, respectively. IR and Raman spectra, obtained over a large temperature range, permit one to obtain a better understanding of inner surface H₂O-molecule behavior in microporous silicates and energetics and the behavior of hydrogen bonding.

Keywords: Raman spectroscopy, IR spectroscopy, natrolite, scolecite, microporous materials, Hydrogen bonding, zeolites, H₂O molecules

INTRODUCTION

Zeolites are used in several technological applications and also comprise an important rock-forming mineral group. Zeolites are used as catalysts, for example, in the cracking of hydrocarbons, in molecular sieving and for use in cation-exchange processes. In nature, they can be found in sedimentary rocks, in low-grade metamorphic assemblages and in various hydrothermal deposits. The chemistry of zeolites with a single cation in the channels (we use here the terminology based on the IUPAC recommendations outlined by McCusker et al. 2001) can be represented by the general formula M_{*x*}[AlO₂]_{*x*}(SiO₂)_{*y*}]·*m*H₂O, where M is a cation of valence *n* and *m* is the number of water molecules in the unit cell (Gottardi and Galli 1985). In terms of their crystal structures zeolites are classified as framework silicates consisting of corner-linked AlO₄ and SiO₄ tetrahedra. To balance the negative charge in the framework, resulting

from the presence of the Al cations, M cations are located in structural channels. The M cation is typically monovalent such as Li⁺ and Na⁺, or divalent such as Mg²⁺ or Ca²⁺, for example. H₂O molecules are also found in the structural channels and are present in different concentrations. H₂O can be easily driven out of the channels by heating zeolites at relatively low temperatures (Cronstedt 1756). Thus, one can readily understand his derivation of the word zeolite, which from the Greek means boiling stone. Smith (1963) offered an early definition as: “a zeolite is an aluminosilicate with a framework structure enclosing cavities occupied by large ions and water molecules, both of which have considerable freedom of movement, permitting ion-exchange and reversible dehydration.”

Herein, we focus on the behavior of the H₂O molecules located in the two fibrous zeolites natrolite, Na₁₆[Al₁₆Si₂₄O₈₀]·16H₂O, and scolecite, Ca₈[Al₁₆Si₂₄O₈₀]·24H₂O. Both natrolite and scolecite can be classified as small-pore zeolites consisting of eight-membered rings having channels around 2.5 × 4 Å in size that are parallel to the crystallographic *c*-axis. Surprisingly, inasmuch as

* E-mail: chg@min.uni-kiel.de

it is the presence of molecules in small channels and their effect on the physical behavior that make the zeolites so interesting and a useful class of silicates, relatively little research has been directed toward the H₂O molecules especially using spectroscopic techniques. In the case of natrolite, Pechar and Rykl (1983) presented IR and Raman spectra and made mode assignments based on lattice-dynamic calculations. Gottardi and Galli (1985) presented powder MIR spectra for natrolite and scolecite, but little spectral interpretation was given. Line and Kearley (1998) measured inelastic neutron scattering spectra and powder MIR spectra of natrolite, and undertook ab-initio calculations, in their analysis of the vibrational behavior of the Na cations and H₂O molecules in the channels. Incoherent inelastic neutron scattering measurements on natrolite and scolecite have also been used to further investigate the low-energy vibrational behavior of their channel species (Line and Kearley 2000). Gunter and Ribbe (1993) related the optical properties of natrolite and scolecite to H₂O content and orientation of the H₂O molecules. There are still, however, little quantitative data and/or understanding of the vibrational, energetic, and bonding properties of H₂O in zeolites as compared, for example, to the voluminous literature on their static crystal structures and crystal-chemical properties (see Armbruster and Gunter 2001; Passaglia and Sheppard 2001 for recent reviews). Much research needs to be done in making mode assignments, for example. Little work has been done in measuring vibrational spectra at different temperatures. The availability of new spectrometers with microscopes and improved detectors allows for high quality vibrational spectra to be measured, and new insight can be obtained.

This work is an extension of, and builds upon, earlier vibrational spectroscopic studies on other hydrous (i.e., hydrophilic) microporous silicates. In the case of beryl and cordierite, where a single H₂O molecule is located in a small microporous cavity, there is little interaction of the H₂O molecule with the silicate framework (Kolesov and Geiger 2000a, 2000b, and references therein). The behavior of H₂O that forms an ordered one-dimensional chain of H₂O molecules in the zeolite bikitiaite was addressed by Kolesov and Geiger (2002). Important questions in the current study include the nature of hydrogen bonding in silicate systems, the energetics of the H₂O molecule in different structural micropores and molecule-inner-surface interactions. In addition, the physical nature of hydrophobic vs. hydrophilic behavior in microporous silicates is of great current interest (e.g., Smith 1998). Such investigations are necessary to obtain a physical understanding of more complicated H₂O-molecule-silicate interactions that occur in nature.

CRYSTAL STRUCTURES AND THE OCCLUDED H₂O MOLECULES IN NATROLITE AND SCOLECTITE

The crystal structures of natrolite and scolecite have been investigated several times using both X-ray and neutron diffraction methods (see Armbruster and Gunter 2001 for a review). Both zeolites are structurally related, belonging to the NAT group of zeolites (Baerlocher et al. 2005). The crystal structure of natrolite (space group *Fdd2*), showing the aluminosilicate framework of corner-linked tetrahedra, is illustrated in Figure 1a. The H₂O molecules and Na cations are located in the channel cavities, related by a 2₁-screw axis at the center of the channel. Each Na

is bonded to four framework O atoms and two H₂O molecules. For each H₂O molecule, the O atom is bonded to two Na atoms, and the two H atoms are hydrogen bonded to two different O atoms of the framework (Fig. 1b).

The structure of scolecite (space group *F1d1*) is shown in Figure 2a. The reduction of symmetry from that of natrolite is related to the difference in the channel content, i.e., in scolecite there is only one Ca and three H₂O molecules (Fig. 2b). Indeed, one Na site in natrolite is replaced by one H₂O molecule (2Na ↔ Ca + H₂O). The Ca cation is bonded to four O atoms of the framework and three O atoms of H₂O molecules. All three H₂O molecules are characterized by slightly different O···H bond lengths and thus have slightly different O-H bond strengths (Kvick et al. 1985).

The H₂O molecules in natrolite and scolecite have C_{1*v*} symmetry (compared to C_{2*v*} for a free H₂O molecule) and occupy general crystallographic positions. Each water molecule forms hydrogen bonds of different strengths with its local surroundings in the cavity. All H₂O vibrational modes, three internal and six external, are active in the IR and Raman.

EXPERIMENTAL METHODS

The natrolite crystal used for Raman study is the same as that used in the neutron diffraction investigation of Artioli et al. (1984). Powder IR spectra were obtained from a single crystal collected from the Kola Peninsula in Russia. The scolecite sample, used for both Raman and IR measurements, was taken from a bundle of crystals about 5 cm in length and 3 mm wide originating from Chalisgaon, Maharashtra, India. All samples are clear, transparent, gem-quality single crystals.

Powder transmission IR measurements were made using a Bruker FT-IFS66 spectrometer equipped with a MCT detector. Between 0.6 and 1.0 mg of zeolite was ground and mixed with about 300 mg KBr and pressed under vacuum to a transparent pellet of 13.0 mm diameter. The low-temperature spectra were recorded using a cold-finger-type He-closed-cycle cryostat attached to the spectrometer. The precision of the temperature control is about ±1 K. Spectra were collected from 300 to 50 K at intervals of 20 or 10 K. A total of 32 scans was recorded at a resolution of 2 cm⁻¹ and merged for the final spectrum.

The Raman spectra were collected using a triple grating spectrometer with a CCD detector. The 488 nm line of an Ar laser was used for the spectral excitation. The low- and room-temperature spectra were measured in 180° collection geometry with a Raman microscope. The low-temperature spectra were recorded by fixing the crystal on a cold finger of a helium cryostat (MicrostatHe) from Oxford Instruments. The precision of the measured temperatures is estimated to be ±1 K. All measurements were performed with a spectral resolution of 2 cm⁻¹ at low temperature (4 K) and 5 cm⁻¹ at other temperatures.

RESULTS

Natrolite

Figures 3a and 3b, respectively, show the 4 K and room-temperature polarized single-crystal Raman spectra of natrolite in the regions of the H₂O internal stretching and bending vibrations. The spectra at 298 K show two main bands at 3324 and 3538 cm⁻¹ and several others of weaker intensity. At 4 K the two main bands are located at 3319 and 3539 cm⁻¹. The only notable difference in the spectra at the two temperatures lies in the behavior of the band at ~3179 cm⁻¹, which is observed at room temperature and not at 4 K. Stacked plots of powder IR and single-crystal Raman spectra at various temperatures (Figs. 4a and 4b) between 4 and 298 K show that this band appears with increasing temperature around 80 K as a weak feature and its intensity becomes greater with increasing of temperature. The bending mode of H₂O in natrolite is present at 1629 cm⁻¹ as a

weak band in the Raman *ac*- and *bc*-spectra (Fig. 3b). In the IR spectra, this band is located at about 1636 cm⁻¹ (Fig. 4a—the other band at ~1670 cm⁻¹ is difficult to assign and may possibly represent a second-order absorption). Figure 5 shows unpolarized Raman spectra of natrolite at temperatures from 295 to 570 K in the region of the H₂O stretching vibrations.

Scolecite

The polarized single-crystal Raman spectra of scolecite at 4 K and room temperature in the range of H₂O stretching and bending regions are shown in Figures 6a and 6b, and the powder IR spectra at different temperatures in Figure 6c. The room temperature IR and Raman spectra show five main H₂O stretching bands. The low temperature Raman spectra, in comparison, show 6 bands (Fig. 6a). The band at 3503 cm⁻¹ at room temperature appears to split into two bands at 3493 and 3498 cm⁻¹ in the 4 K spectra. Figure 6b shows three H₂O bending vibrations at room temperature. Three bending modes are also observed in the IR. Because the intensity of the bending modes in cross polarization gives the orientation of the molecular plane, mode assignments for the bending vibrations in Figure 6b can be made.

Figure 7a shows unpolarized Raman spectra of the stretching vibrations at elevated temperatures from 295 to 720 K. The bands are broadened and strongly overlapped at $T > 470$ K. Ståhl and Hanson (1994) showed that the dehydration of scolecite starts at approximately 313 K with expulsion of one of the three water molecules, labeled W2 (Fig. 2b), at temperatures around 473 K. When approximately 50% of the W2 molecules are expelled, scolecite undergoes a phase transition. Figure 7b shows the integrated intensity of the O-H stretching bands in the temperature range of 400–470 K. The band at ~3230 cm⁻¹ does not change in intensity, whereas the two bands at ~3410 and 3510 cm⁻¹ increase, and the two remaining bands at ~3330 and ~3570 cm⁻¹ decrease in intensity upon heating. Note that the integrated intensity of the individual bands was obtained by fitting Lorentzian components to the band envelope. As shown below, there are several weak intensity combination modes located between the intense bands. They can be identified through decomposition of the low-temperature spectra. For this reason, the calculated integrated intensities include the intensity of weak neighboring combination band(s).

DISCUSSION

Spectral analysis and H₂O mode assignments: Natrolite

Two intense O-H stretching modes are observed in the IR and Raman spectra of natrolite (Fig. 3). The low-wavenumber mode at ~3320 cm⁻¹ represents to a large degree the motion of the more strongly H-bonded hydrogen atom of the H₂O molecule. The high-wavenumber band at ~3540 cm⁻¹ is related to an O-H mode related to the more weakly H-bonded hydrogen atom. The former mode derives from the ν_1 mode of a free symmetric H₂O molecule and the latter from the asymmetric vibration, ν_3 . This assignment can be made from a consideration of the wavenumber behavior of OH modes as a function of hydrogen bonding strength (e.g., Libowitzky 1999). The mode at ~3320 cm⁻¹ is strong in the Raman *bb*-spectrum, whereas the mode at ~3540 cm⁻¹ is strong in the *aa*-spectrum (Fig. 3). This is consis-

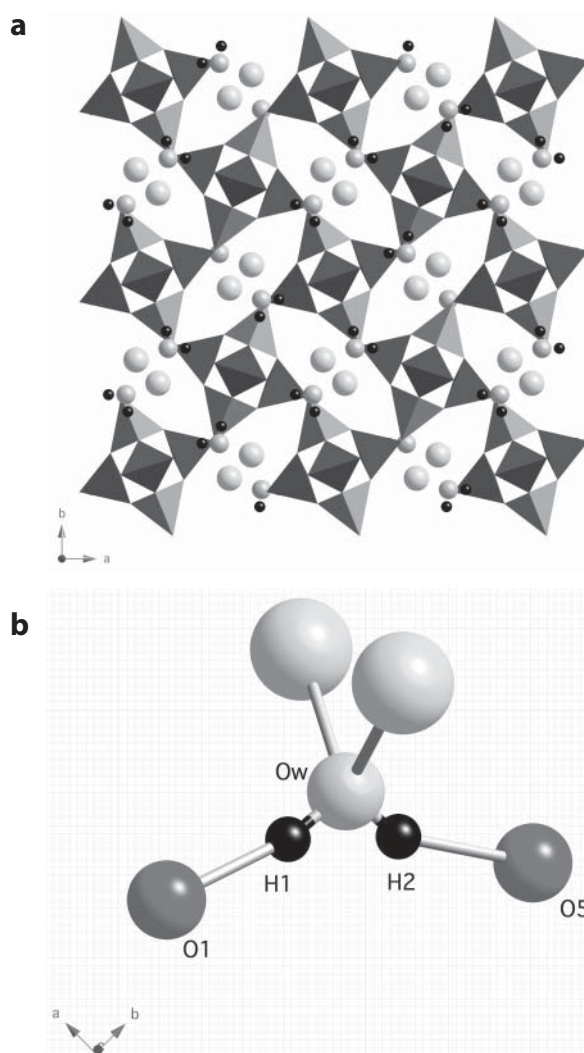


FIGURE 1. (a) Crystal structure model of natrolite, *Fdd2*, projected down the *c*-axis. In the channels one can observe two Na cations, which are related by the 2_1 -screw axis along [001] in the center of the channel, and the H₂O molecules that are located closer to the channel walls. (b) The local bonding environment of a H₂O molecule in natrolite. Its oxygen (Ow) is bonded to two Na cations, and the hydrogen atoms (H1 and H2) are hydrogen bonded to two different framework O atoms. The atomic coordinates and labels are taken from Artioli et al. (1984).

tent with the orientation of the O-H bonds of the H₂O molecule in the channel micropores, where the shorter (0.964 Å) Ow-H2 bond of the H₂O molecule (i.e., weakly hydrogen bonded) is located in *ac*-plane of the crystal and the longer Ow-H1 (0.974 Å—more strongly hydrogen bonded) bond is located in the *bc*-plane (Artioli et al. 1984; see Fig. 1b).

The band at 3218 cm⁻¹ at 4 K (Fig. 3a) represents a Fermi-resonanced double bending mode of H₂O. The wavenumber of the bending mode is ~1630 cm⁻¹ at 298 K (Figs. 3a and 4a).

The band at 3469 cm⁻¹ in the Raman *bb*-spectrum at room temperature (Fig. 3b) and in the IR spectra (Fig. 4a) is separated from the intense Ow-H1 stretching band at ~3320 (3324 cm⁻¹

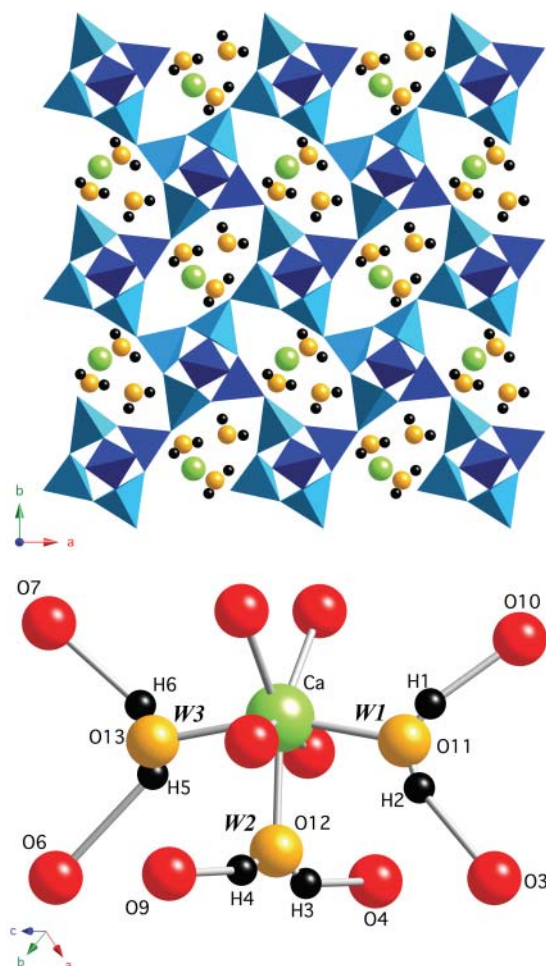


FIGURE 2. (a) Crystal structure model of scolectite, *F1d1*, projected down the *c*-axis. The atomic coordinates are taken from Stuckenschmidt et al. (1997). Each channel contains one Ca cation and three H₂O molecules that are located closer to the channel walls. (b) The bonding relationship for the “Ca-cluster” in scolectite showing the three H₂O molecules and O atoms from the framework. The O atoms of the three molecules are bonded to the Ca cation, and the H atoms of the H₂O molecules are hydrogen bonded to different framework O atoms. The atom and H₂O molecule (*W1*, *W2*, and *W3*) labels are from Kvik et al. (1985).

at room temperature) by 146 cm⁻¹. The band at 3179 cm⁻¹ (Fig. 3b) first appears in both Raman and IR spectra at temperatures greater than 80 K (Figs. 4a and 4b) and is separated from the band at 3320 cm⁻¹ by approximately the same value, 144 cm⁻¹, but is located at lower energies. Thus, we interpret these two weak Raman bands as “Stokes” (3469 cm⁻¹) and “anti-Stokes” (3179 cm⁻¹) counterparts of the same combination mode [i.e., $\nu_{\text{O-H}} + T(\text{H}_2\text{O})$ and $\nu_{\text{O-H}} - T(\text{H}_2\text{O})$], which results from a coupling between a low-wavenumber external H₂O translational mode [*T*(H₂O)] at about 145 cm⁻¹ and the Ow-H1 stretching mode.

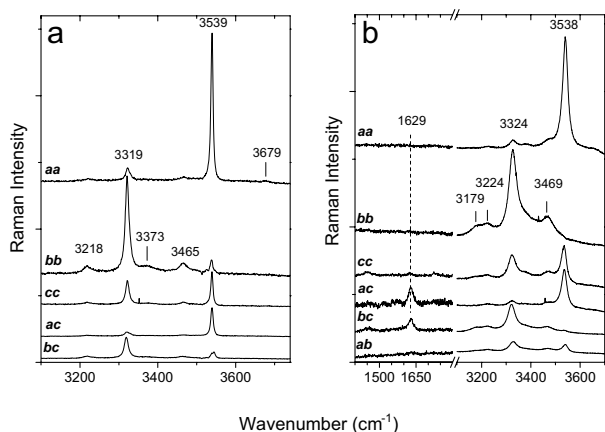


FIGURE 3. (a) 4 K and (b) room-temperature polarized single-crystal H₂O Raman spectra of natrolite in the range of H₂O stretching (and bending) vibrations.

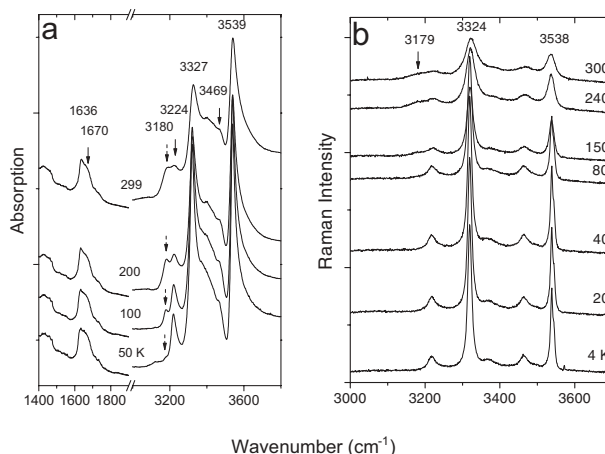
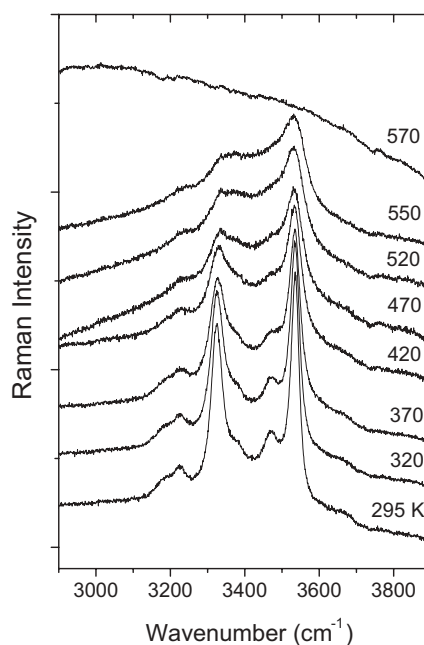


FIGURE 4. (a) Infrared and (b) Raman spectra of natrolite at temperatures between 4 and 300 K.



► **FIGURE 5.** Unpolarized Raman spectra of natrolite at elevated temperatures in the wavenumber region of the H₂O stretching vibrations.

The temperature dependence of the intensity of the mode at 3179 cm⁻¹ is governed by Boltzmann statistics, i.e., by the thermal population of the excited vibrational state.

Note that the band at 3469 cm⁻¹ is not a single combination mode. A deconvolution into Lorentzian components produces weak features at approximately 3369, 3392, 3426, and 3495 cm⁻¹ (not shown here) in the unpolarized Raman and IR spectra. The effect of temperature broadening hinders an observation of their anti-Stokes counterparts because of the presence of the strong OH band at 3324 cm⁻¹, and we cannot, at this point, determine them. Possibly, these weak features are also combination modes of internal-external H₂O vibrations, but an assignment to triple overtone vibrations of Si-O stretching modes cannot be ruled out.

The energies of hindered translational modes of H₂O molecules in liquid water lie in the range of 0–200 cm⁻¹, whereas librational modes are found in the range of 300–900 cm⁻¹ (Eisenberg and Kauzmann 1969). Thus, the mode at about 145 cm⁻¹ should be assigned to a hindered translational motion of the H₂O molecule that is hydrogen bonded with the framework. A mode at 145 cm⁻¹ (18 meV) was also observed, among others, in inelastic incoherent neutron scattering spectra by Line and Kearley (2000), but they assigned it to an H₂O-Na stretching vibration. One should note, however, that O-H stretching modes in Raman (and IR) spectra combine primarily with vibrations of the bonds that are modulated during the displacement of the hydrogen atom (i.e., the hydrogen bond, O-H···O). Therefore, our assignment of the mode at 145 cm⁻¹ to an H-bonded H₂O molecule translation, we believe, is correct. It is of interest to note that an analogous combination mode is observed on the high-wavenumber side of the intense Ow-H2 stretching band at 3540 cm⁻¹ (i.e., the weak band at 3679 cm⁻¹ in the *aa*-spectrum; Fig. 3a), but its intensity

is much weaker than that at 3469 cm⁻¹. The weak intensity can be explained by the fact that combination modes having vibrational transitions with a change in the vibrational quantum number of ± 2 are forbidden in infrared absorption or Raman scattering. Thus, their appearance results from anharmonic interactions between vibrations. Following this argumentation, the greater intensity of the combined H₂O translation and the Ow-H1 stretching mode reflects a stronger anharmonicity of the OH1···O hydrogen bond than that associated with the O-H2···O hydrogen bond.

Temperature behavior

Figures 8a–d show wavenumber variations of several internal H₂O modes and the external H₂O translational mode (145 cm⁻¹) as a function of temperature. The wavenumbers of the two intense H₂O stretching modes at 3320 and 3540 cm⁻¹ vary in opposite directions with changing temperature. The mode at 3320 cm⁻¹ decreases in energy with decreasing temperature, whereas the mode at 3540 cm⁻¹ increases. Because the magnitude of the wavenumber shifts is the same for both modes, i.e., ~ 4 cm⁻¹ between 300 and 4 K, this behavior is probably a manifestation of the internal properties of the H₂O molecule and does not result from a change in the strength of hydrogen bonding of the H₂O molecule with the framework oxygen atoms. (A detailed analysis of this problem is beyond the scope of this study.)

The wavenumber of the translational mode, $T_{\text{H}_2\text{O}}$, which is derived from the combination mode [(Ow-H1) + $T_{\text{H}_2\text{O}}$] at 3469 cm⁻¹, decreases very slightly in wavenumber upon cooling (Fig. 8d). That is, its energy, which is a function of both (Ow-H1)···O and (Ow-H2)···O force constants, decreases very slightly with decreasing temperature. This observation permits one to differentiate a combination mode that contains a low-energy external H₂O mode from a lattice vibration. The latter typically increases

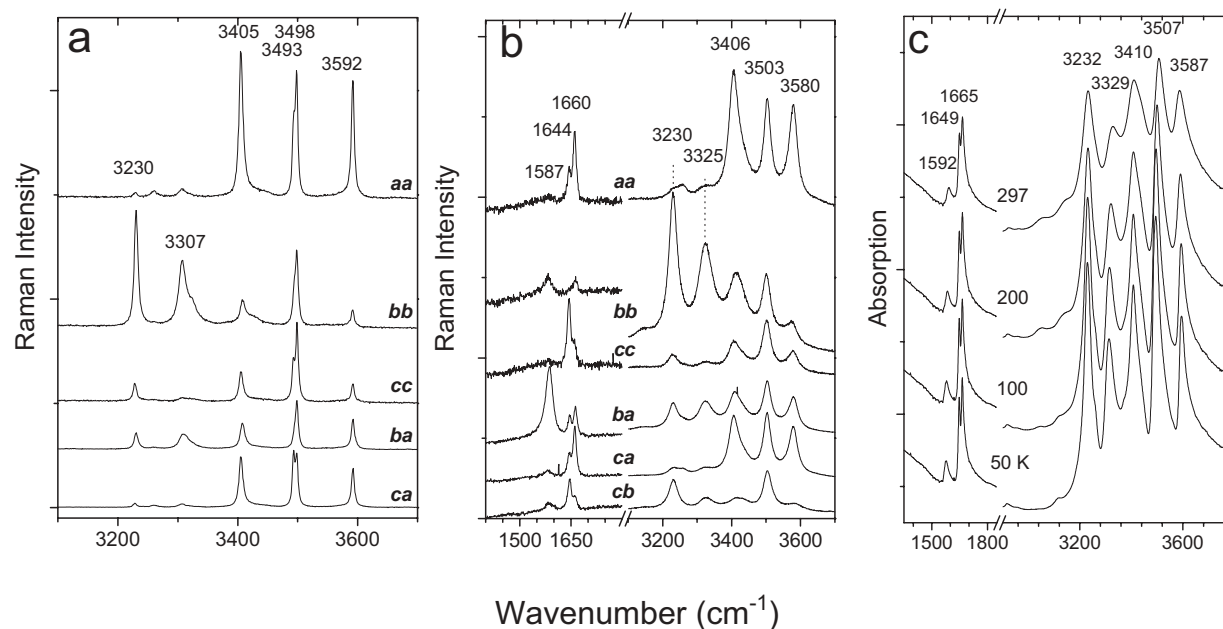


FIGURE 6. (a) Polarized Raman spectra of scolecite at 4 K and (b) room temperature. (c) Infrared spectra in the range of OH stretching and bending vibrations between 50 and 298 K.

in energy upon cooling, because their force constants increase.

Figure 9a shows the Raman *aa*-spectra of natrolite, containing several lattice vibrations, at room temperature and 4 K (The spectra are only shown between 80 and 640 cm⁻¹ to allow a better

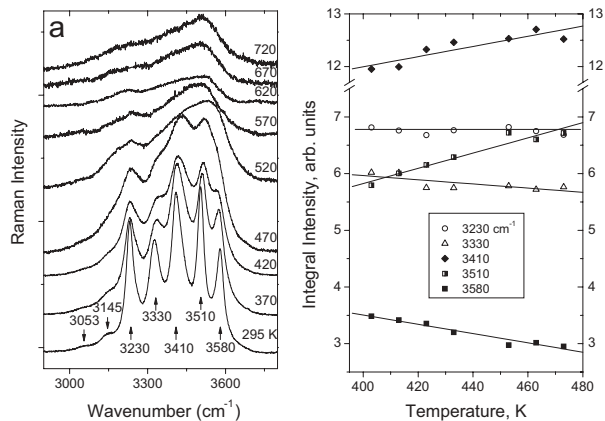


FIGURE 7. (a) Unpolarized Raman spectra of scolectite at elevated temperature and (b) temperature behavior of the integral intensity of the stretching H₂O modes.

comparison of the two spectra at the two different temperatures. The higher wavenumber lattice modes show a typical increase in wavenumber upon cooling and are not shown). In contrast, the band at ~143 cm⁻¹ has a slightly lower wavenumber at 4 K compared to RT. The energy of this mode is similar to that determined from an analysis of the combination modes located in the OH stretching vibration region. In addition to this low-energy mode, a mode at 110 cm⁻¹ in the (*ac*)-spectrum (not shown here) also has a lower wavenumber at 4 K than at 298 K and it should, in addition, be assigned to an H₂O translation. Both of these modes were observed and attributed to H₂O translations by Line and Kearley (1998), and the mode at 144 cm⁻¹ was recorded in the Raman spectra of Goryainov and Smirnov (2001).

The strong mode at ~440 cm⁻¹ in the (*aa*)-spectra at 4 K (Fig. 9a) and a mode at 496 cm⁻¹ in the (*bb*)-spectra (at room temperature and not shown here) show a similar temperature behavior as the mode at 144 cm⁻¹. Because they have higher energies than the H₂O-translation modes and because they show a decrease in energy upon cooling, we propose that both of these modes are related to H₂O librations. However, an assignment to H₂O-Na vibrations also should be considered. (The band at ~440 cm⁻¹ consists of two modes at room temperature, and more work is required to understand the phenomena).

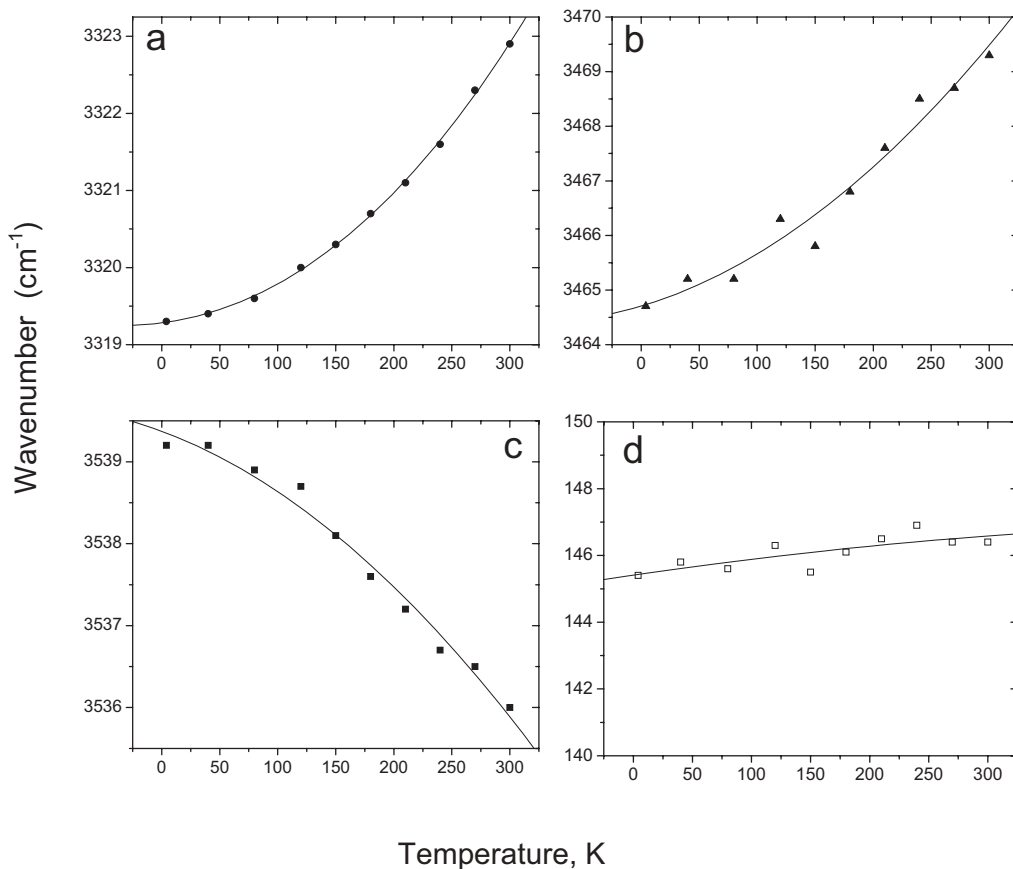


FIGURE 8. Wavenumber dependence of H₂O stretching and combined modes as a function of temperature in natrolite: (a) Mode at 3320, (b) 3465, (c) 3540 cm⁻¹, and (d) difference between the modes at 3465 and 3320 cm⁻¹.

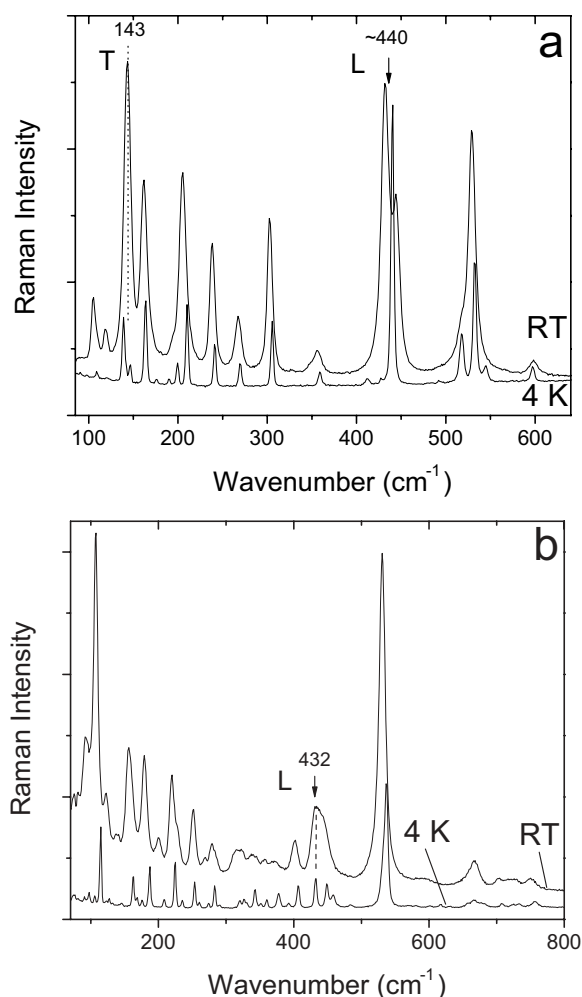


FIGURE 9. (a) Raman (*aa*)-spectrum of natrolite and (b) scolecite at 4 K and room temperature.

TABLE 1. Raman bands in the wavenumber region of their O-H stretching vibrations [$\nu(\text{OH})$] in scolecite and their assignment

| $\nu(\text{OH})$ (cm^{-1}) | $T = 4 \text{ K}$ | 3230 | 3307 | 3405 | 3493 | 3498 | 3592 |
|---------------------------------------|---------------------|--------|--------|--------|--------|--------|--------|
| | $T = 403 \text{ K}$ | 3231 | 3333 | 3410 | 3510 | 3510 | 3573 |
| Assignment | | O11-H1 | O12-H3 | O13-H6 | O13-H5 | O11-H2 | O12-H4 |
| Distance (\AA)* | O-H | 0.9755 | 0.9694 | 0.9706 | 0.967 | 0.9638 | 0.9497 |
| | O...O | 2.7204 | 2.6568 | 2.7854 | 3.0457 | 3.0458 | 2.7555 |

* Kvik et al. (1985).

Scolecite: Internal H₂O modes

The spectra of scolecite can be analyzed using published diffraction results and a consideration of hydrogen-bond behavior in crystal hydrates. The three crystallographically distinct H₂O molecules in each cavity have different hydrogen bond lengths with neighboring framework O atoms (Kvik et al. 1985; Fig. 2b). Thus, one should observe six O-H stretching vibration bands as seen in the Raman spectra at 4 K (Figs. 6a and 6b). However, an assignment of all the modes located between 3200 and 3600 cm^{-1} is not a simple task, because the three H₂O molecules give rise to a complicated system of interacting vibrations (i.e., stretching-

stretching, stretching-translational, and translational-translational H₂O modes). For our analysis and mode assignments, we will use the notation for the atoms and bonds of the H₂O molecules as found in Kvik et al. (1985) and the crystal axes (i.e., structural convention) from Stuckenschmidt et al. (1997).

The intensity of the two bands at ~ 3330 and ~ 3580 (or 3587 in the IR) cm^{-1} at room temperature (3307 and 3592 cm^{-1} respectively at 4 K; Figs. 6a, 6b, and 6c) decrease most strongly upon heating (Fig. 7b) in the temperature range of 403–473 K. Both powder X-ray and thermal analysis measurements indicate that the W2 (H3-O12-H4) molecule (Fig. 2b) is the first molecule that begins to diffuse out of the crystal, followed by W1 and W3 at higher temperatures (Gottardi and Galli 1985; Ståhl and Hanson 1994). Hence, the band at 3307 cm^{-1} (Fig. 6a) is assigned to a stretching vibration of the O12-H3 bond and the band at 3592 cm^{-1} to that of O12-H4. The O12-H3 bond is directed along the *b*-axis and the O12-H4 bond along the *a*-axis. This is consistent with the intensity of these bands in the polarized Raman spectra (Fig. 6a). As for the other OH bands, a consideration of the relationships between band wavenumber and OH bond length (i.e., Libowitzky 1999), on the one hand, and between band intensity in the polarized spectra and crystallographic bond orientation, on the other hand, allows mode assignments to be made. Thus, the bands at 3230 and 3498 cm^{-1} are assigned to vibrations of the W1 molecule (H1-O11-H2) and the bands at 3405 and 3493 cm^{-1} to the vibrations of the W3 molecule (H5-O13-H6). The final mode assignments, together with O-H and O...O distances, are given in Table 1. The data in Table 1 show a satisfactory correlation between $\nu(\text{OH})$ and the O-H distance but a poor correlation between $\nu(\text{OH})$ and the O...O distance. The latter is due to the affect of the O-H...O angle, which deviates from 180° in many zeolites (Kvik et al. 1985). Therefore, in contrast to other hydrous microporous silicates, the O...O distance is not a good criterion for making OH band assignments in scolecite.

The room-temperature Raman spectra show three H₂O bending modes, ν_2 , at 1587, 1644, and 1660 cm^{-1} (Fig. 6b). The IR spectra are similar in this regard. The polarization vectors of the incident and scattering light in the Raman experiment form a plane and the bending mode is most intense when the H₂O molecule lies within it, thus defining its orientation. The mode at 1587 cm^{-1} is most intense in the Raman *ab*-spectrum (Fig. 6b) and is, therefore, assigned to the H3-O12-H4 (W2) bending vibration (Fig. 2b). The other two ν_2 modes at 1644 and 1660 cm^{-1} are attributed to W1 and W3 molecules, respectively.

Combination bands and external H₂O modes

An analysis of the H₂O-related combination modes in the spectra of scolecite, which consist of internal O-H stretching and external H₂O modes, is complicated. An attempt will be made to assign the various bands using the Raman (*bb*)-spectra (Fig. 10). First, the very weak bands located at 3116 and 3260 cm^{-1} , appearing in spectra with different polarizations (Figs. 6 and 10), should be assigned to double frequency Fermi-resonance modes consisting of different bending vibrations of H₂O. The other weak bands in the low temperature (*bb*)-spectrum, i.e., 3323, 3384, 3423, 3458, 3544, and 3568 cm^{-1} (Fig. 10) are considered true combination modes. The weak broad bands that are present in the temperature range of 80–295 K, but are absent in the

spectrum at 4 K, i.e., modes at 3053 and 3145 cm⁻¹ in Figure 10, are anti-Stokes counterparts of some of the combination bands listed above. To have measurable Raman mode intensity at $T \leq 300$ K, the energy of the external H₂O modes involved in the anti-Stokes vibrations should be less than about 200 cm⁻¹. Based on this observation, the bands at 3053 and 3145 cm⁻¹ in the RT-spectrum should be assigned to combined $\nu(\text{OH})\text{-}T_{\text{H}_2\text{O}}$ modes, consisting of the stretching vibration $\nu(\text{O11-H1}) = 3231$ cm⁻¹ and the external translation vibrations $T_{\text{H}_2\text{O}(W1)} = 178$ and 86 cm⁻¹, respectively. In the Stokes part of the Raman spectra, their counterparts overlap the intense OH bands at 3306 (O12-H3) and 3408 (O13-H6) cm⁻¹ and couple with them giving rise to the relatively intense bands located at 3323 and 3423 cm⁻¹, respectively. The very weak bands at 3343, 3384, and 3458 cm⁻¹ could also represent combined modes consisting of translational H₂O modes and the intense OH modes at 3231 and 3306 cm⁻¹, but we cannot verify this. The band at 3544 cm⁻¹ can be assigned to a translational H₂O mode combined with the O-H stretching mode at 3499 cm⁻¹ (O11-H2). This third translational mode should have an energy of 45 cm⁻¹. The band at 3568 cm⁻¹ is assigned to a combination mode consisting of $T_{\text{H}_2\text{O}}$ with the OH stretching modes at 3408 or 3499 cm⁻¹. However, it is not possible to observe their anti-Stokes counterparts due to broadening and overlapping of OH bands at temperatures greater than 100 K. We are not able to identify with certainty pure H₂O translational modes in the low-wavenumber regions (Fig. 9b).

The spectra of scolecite, which are similar to those for natrolite, show broad bands around 430 cm⁻¹ in the *aa*-spectra (Fig. 9b) and also in the *bb*- and *cc*-spectra (not shown here). In addition, bands at 490 (*ab*-spectra) and 667 cm⁻¹ (*ac*-spectra) can also be observed, but the spectra are not shown here. They are assigned to H₂O librations, $R_{\text{H}_2\text{O}}$, or cation-H₂O translations, because their line widths at room temperature are measurably greater compared to those of the lattice modes. However, it is difficult to determine which of the three H₂O molecules (W1, W2, or W3) relate to these bands.

As for the inelastic incoherent neutron scattering spectra of scolecite from Line and Kearley (2000), only their band at 81 cm⁻¹ (10 meV) is also observed in our Raman spectra. The other external H₂O modes reported by them have energies that are different from those determined from our analysis for reasons that are not clear to us.

DEHYDRATION BEHAVIOR

Natrolite

Upon heating natrolite, all OH bands become broader and weaker, as the amount of H₂O in the channels decreases (Fig. 5). Above 570 K there is no measurable H₂O in the crystal. The spectra are in good agreement with the thermal gravimetry and differential thermal analysis results given by Gottardi and Galli (1985).

Scolecite

The behavior of OH modes in scolecite at elevated temperatures (Fig. 7) was discussed partly above. Two further aspects should be considered: (1) the relative increase in intensity of the bands at ~3410 and 3510 cm⁻¹ with increasing temperature, and

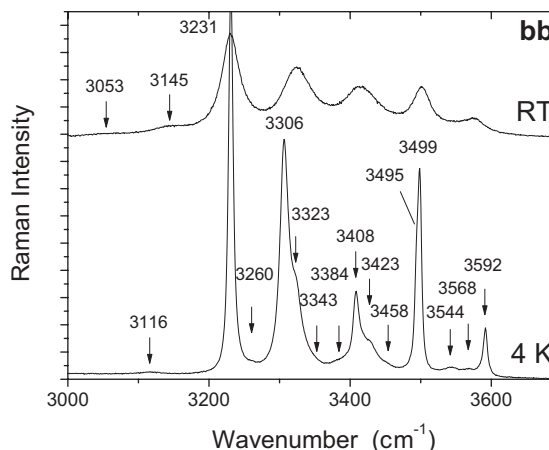


FIGURE 10. Raman (*bb*)-spectra of H₂O stretching and combined modes in scolecite at 4 K and room temperature.

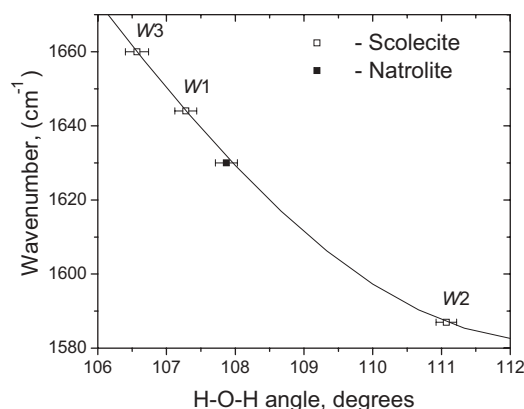


FIGURE 11. Wavenumber of the H₂O bending vibration as a function of the H-O-H angle for the H₂O molecules in scolecite and natrolite. The angles are taken from the neutron diffraction results of Kvik et al. (1985) for scolecite, and Artioli et al. (1984) for natrolite.

(2) the intensity weakening of the bands at ~3330 and ~3580 cm⁻¹. The anti-Stokes combination modes at 3053 and 3145 cm⁻¹ only change slightly in energy with temperature, and this behavior is unlike the behavior of normal modes. A possible reason for this is that the translational modes associated with the three H₂O molecules are coupled (Fig. 2b), and a decrease in concentration of the W2 H₂O molecules causes a change in the translational energies associated with the W1 and W3 H₂O molecules. Accepting this proposal, the assignments and temperature behavior of the other vibrational modes can be interpreted. The combined Stokes modes for the W1 H₂O molecule overlap the OH stretching modes related to the W2 and W3 molecules (i.e., the modes at ~3330 and ~3410 cm⁻¹, respectively). When the W1 H₂O molecule diffuses out upon heating, the coupling conditions change and this leads to an increase in the intensity of the modes at ~3330 and ~3410 cm⁻¹.

On the other hand, the intensity of the OH band at 3330 cm⁻¹ that is related to W2 should become weaker due to the loss of H₂O

TABLE 2. Wavenumber of the O-H stretching ($\nu_{\text{O-H}}$) and translation vibrations [$T(\text{H}_2\text{O})$] of the H₂O molecule (cm^{-1}) in liquid water and various microporous hydrous silicates

| Liquid water* | | Beryl† | | Bikitaite‡ | | Natrolite | | Scolecite (W1) | |
|--------------------|-------------------------|--------------------|-------------------------|--------------------|-------------------------|--------------------|-------------------------|--------------------|-------------------------|
| $\nu_{\text{O-H}}$ | $T(\text{H}_2\text{O})$ | $\nu_{\text{O-H}}$ | $T(\text{H}_2\text{O})$ | $\nu_{\text{O-H}}$ | $T(\text{H}_2\text{O})$ | $\nu_{\text{O-H}}$ | $T(\text{H}_2\text{O})$ | $\nu_{\text{O-H}}$ | $T(\text{H}_2\text{O})$ |
| 3200-3400 | ~180° | 3605 | 9 | 3372 | 130 | 3319 | 145 | 3230 | 45 |
| | | | | 3597 | | 3539 | | 3498 | 86 |
| | | | | | | | | | 178 |

* Afsar and Hasted (1977).

† Kolesov and Geiger (2000a).

‡ Kolesov and Geiger (2003).

at elevated temperatures. However, the changes in the intensity of this band are the sum of two different effects and are less than that which would result just from a decrease in the concentration of W2-H₂O alone (Fig. 7b). Similar behavior governs the intensity of the other OH modes also.

BENDING MODE BEHAVIOR AND H₂O GEOMETRY

Based on the measured spectra and structural data obtained from neutron-diffraction measurements on scolecite and natrolite at low temperature (Kvick et al. 1985; Artioli et al. 1984), one can describe the dependence of the ν_2 wavenumber as a function of the H-O-H angle (Fig. 11). At first glance, a physical explanation for the resulting relationship is not clear. Based on simple molecular dynamic considerations, the wavenumber of ν_2 for H₂O in a mineral such as scolecite should tend to the ν_2 value for a free H₂O molecule (i.e., 1595 cm^{-1} ; Eisenberg and Kauzmann 1969), when the H-O-H bond angle approaches the value found in an H₂O molecule (i.e., 104.8°). Instead, an inverse relationship is observed (Fig. 11). Moreover, with an increase in the strength of hydrogen bonding, i.e., for W2, the ν_2 wavenumber should increase as well based on various experimental and theoretical considerations (see e.g., Falk 1984). Instead, once again, an inverse relationship is observed. On the other hand, in the case of beryl and cordierite, the wavenumber of ν_2 for Type II H₂O, which is bonded to an alkali cation, is greater than the wavenumber of ν_2 associated with Type I H₂O (Wood and Nassau 1968; Charoy et al. 1996; Goldman et al. 1977). Evidently, the studies show that when a non-H-bonded H₂O molecule is bonded to a cation, this leads to an increase in the wavenumber of ν_2 , which contradicts the analysis of Falk (1984) and Falk et al. (1986).

One can propose, therefore, that the wavenumber behavior of ν_2 (Fig. 11) for scolecite and natrolite is a function of the bonding behavior of the H₂O molecule to a Ca²⁺ atom or two Na⁺ cations. If we assume that the effect of hydrogen bonding on the H₂O molecules in scolecite and natrolite have roughly the same effect on the energy of ν_2 , then the observed wavenumber trend is understandable. The H-H coulomb interaction and the force constant of the bending vibration should decrease with an increase in the H-O-H angle (i.e., the force constant is proportional to $d_{\text{H-H}}^{-2}$ and the wavenumber of ν_2 to $d_{\text{H-H}}^{-1}$, where $d_{\text{H-H}}$ is the distance between the two H atoms). The curve in Figure 11 is obtained by fitting the function $d_{\text{H-H}}^{-1} = [2d_{\text{O-H}} \sin(\alpha/2)]^{-1}$, where α is the H-O-H angle of the H₂O molecule, to the wavenumber of ν_2 for the H₂O molecules in scolecite and natrolite. This relationship demonstrates various aspects about the nature of ν_2 and can be used to estimate the H-O-H angle of H₂O in crystals from spectroscopic measurements.

COMPARISON TO OTHER HYDROUS MICROPOROUS SILICATES AND IMPLICATIONS FOR OTHER SYSTEMS

The strength of hydrogen bonding in natrolite and scolecite is “intermediate” between that in beryl and cordierite, where hydrogen bonding of the quasi-free H₂O molecule is weak to nonexistent (Kolesov and Geiger 2000a, 2000b), and that in bikitaite (Kolesov and Geiger 2002; H₂O molecules in a one-dimensional chain) and hemimorphite (Libowitzky and Rossman 1997; with a single planar H₂O molecule), where the H₂O molecules are H-bonded.

Various spectral properties (i.e., wavenumber, bandwidth, band intensity, and temperature dependencies of both internal and external H₂O vibrational modes), obtained from published works, can be used to build an “H₂O-molecule-mineral database” that serves to describe the nature of H-bonded H₂O-molecule properties in different surroundings (Table 2). Such a “database,” and the physical understanding that it can provide, provides a useful first step in investigating more complicated systems where hydrogen bonding plays an important role, such as in liquid H₂O, geological fluid-mineral systems or even perhaps H₂O in biological systems. The nature of hydrophobic and hydrophilic behavior is also of possible importance in biomineralogical processes (e.g., Smith 1998).

It is interesting to note further that most (nearly all?) microporous silicates are hydrophilic, whereas the microporous silicate melanophlogite is hydrophobic (Kolesov and Geiger 2003). This may be related to the respective nature of the charge distribution in the various silicate frameworks and the molecular polarity (e.g., Nakamoto and Takahashi 1982; Line and Kearley 2000). The H₂O molecule is polar, and it is readily incorporated in many microporous silicates, whereas melanophlogite (also ZSM-5 or silicalite; Flanigen et al. 1978) behaves very differently.

ACKNOWLEDGMENTS

We thank G. Artioli for the donation of the natrolite single crystal and U. Cornelissen for undertaking the IR measurements. F. Liebau and M. Gunter proofread the manuscript and made helpful suggestions to improve the presentation.

REFERENCES CITED

- Afsar, M.N. and Hasted, J.B. (1977) Measurements of the optical constants of liquid water and water-d₂ between 6 and 450 cm^{-1} . *Journal of the Optical Society of America*, 67, 902–904.
- Armbruster, T. and Gunter, M.E. (2001) Crystal structures of natural zeolites. In D.L. Bish and D.W. Ming, Eds., *Natural Zeolites: Occurrence, Properties, Applications*, 45, p. 1–67. *Reviews in Mineralogy and Geochemistry*, Mineralogical Society of America, Chantilly, Virginia.
- Artioli, G., Smith, J.V., and Kvick, Å. (1984) Neutron diffraction study of natrolite, Na₂Al₂Si₄O₁₀·2H₂O, at 20 K. *Acta Crystallographica*, C40, 1658–1662.
- Baerlocher, C., Meier, W.M., and Olson, D.H. (2005) *Atlas of Zeolite Framework Types* (5th edition—www.iza-structure.org/databases/).
- Charoy, B., de Donato, P., Barres, O., and Pinto-Coelho, C. (1996) Channel oc-

- cupancy in alkali-poor beryl from Serra Branca (Goias, Brazil): spectroscopic characterization. *American Mineralogist*, 81, 395–403.
- Cronstedt, A.F. (1756) Om en obekant berg art, som kallas Zeolites (English Translation: On a Unknown Mineral-Species called Zeolites). Kungliga Svenska Vetenskapsakademien, Stockholm, 17, 120–123.
- Eisenberg, D. and Kauzmann, W. (1969) The structure and properties of water. Oxford University Press, Oxford.
- Falk, M. (1984) The frequency of the H-O-H bending fundamental in solids and liquids. *Spectrochimica Acta*, 40A, 43–48.
- Falk, M., Flakus, H.T., and Boyd, R.J. (1986) An ab initio CSF calculation of the effect of water-anion and water-cations on the vibrational frequencies of water. *Spectrochimica Acta*, 42A, 175–180.
- Flanigen, E.M., Bennett, J.M., Grose, R.W., Cohen, J.P., Patton, R.L., Kirchner, R.M., and Smith, J.V. (1978) Silicalite, a new hydrophobic crystalline silica molecular sieve. *Nature*, 271, 512–516.
- Goldman, D.S., Rossman, G.R., and Dollase, W.A. (1977) Channel constituents in cordierite. *American Mineralogist*, 62, 1144–1157.
- Goryainov, S.V. and Smirnov, M.B. (2001) Raman spectra and lattice-dynamical calculations of natrolite. *European Journal of Mineralogy*, 13, 507–519.
- Gottardi, G. and Galli, E. (1985) *Natural Zeolites*, 409 p. Springer-Verlag, Berlin.
- Gunter, M.E. and Ribbe, P.H. (1993) Natrolite group zeolites: Correlations of optical properties and crystal chemistry. *Zeolites*, 13, 435–440.
- Kolesov, B.A. and Geiger, C.A. (2000a) A single-crystal Raman study of the orientation and vibrational states of molecular water in synthetic beryl. *Physics and Chemistry of Minerals*, 27, 557–564.
- — — (2000b) Cordierite II: The role of CO₂ and H₂O. *American Mineralogist*, 85, 1265–1274.
- — — (2002) Raman spectroscopic study of H₂O in bikitaite: “one-dimensional ice.” *American Mineralogist*, 87, 1426–1431.
- — — (2003) Molecules in the SiO₂-clathrate melanophlogite: A single-crystal Raman study. *American Mineralogist*, 88, 1364–1368.
- — — (2005) The vibrational spectrum of synthetic hydrogrossular (Katoite) Ca₃Al₂(O₄H₄)₃: A low temperature IR and Raman spectroscopic study. *American Mineralogist*, 90, 1335–1341.
- Kvick, Å., Ståhl, K., and Smith, J.V. (1985) A neutron diffraction study of the bonding of zeolitic water in scolecite at 20 K. *Zeitschrift für Kristallographie*, 171, 141–154.
- Libowitzky, E. (1999) Correlation of O-H stretching frequencies and O-H...O hydrogen bond lengths in minerals. *Monatshefte für Chemie*, 130, 1047–1059.
- Libowitzky, E. and Rossman, G.R. (1997) IR spectroscopy of hemimorphite between 82 and 373 K and optical evidence for a low-temperature phase transition. *European Journal of Mineralogy*, 9, 793–802.
- Line, C.M.B. and Kearley, G.J. (1998) The librational and vibrational spectra of water in natrolite, Na₂Al₂Si₃O₁₀·2H₂O compared with ab-initio calculations. *Chemical Physics*, 234, 207–222.
- — — (2000) An inelastic incoherent neutron scattering study of water in small-pored zeolites and other water-bearing minerals. *Journal of Chemical Physics*, 112, 9058–9067.
- McCusker, L.B., Liebau, F., and Engelhardt, G. (2001) Nomenclature of structural and compositional characteristics of ordered microporous and mesoporous materials with inorganic hosts. *Pure and Applied Chemistry*, 73, 381–394.
- Nakamoto, H. and Takahashi, H. (1982) Hydrophobic natures of zeolite ZSM-5. *Zeolites*, 2, 67–68.
- Passaglia, E. and Sheppard, R.A. (2001) The crystal chemistry of zeolites. In D.L. Bish and D.W. Ming, Eds., *Natural Zeolites: Occurrence, Properties, Applications*, 45, p. 69–116. Reviews in Mineralogy and Geochemistry, Mineralogical Society of America, Chantilly, Virginia.
- Pechar, F. and Rykl, D. (1983) Study of the vibrational spectra of natural natrolite. *Canadian Mineralogist*, 21, 689–695.
- Smith, J.V. (1963) Structural classification of zeolites. *Mineralogical Society of America Special Paper* 1, 281–290.
- — — (1998) Biochemical evolution. I. Polymerization on internal, organophilic silica surfaces of dealuminated zeolites and feldspars. *Proceedings of the National Academy of Sciences*, 95, 3370–3375.
- Ståhl, K. and Hanson, J. (1994) Real-time X-ray synchrotron powder diffraction studies of the dehydration processes in scolecite and mesolite. *Journal of Applied Crystallography*, 27, 543–550.
- Stuckenschmidt, E., Joswig, W., Baur, W.H., and Hofmeister, W. (1997) Scolecite, Part I: Refinement of high-order data, separation of internal and external vibrational amplitudes from displacement parameters. *Physics and Chemistry of Minerals*, 24, 403–410.
- Wood, D. L. and Nassau, K. (1968) The characterization of beryl and emerald by visible and infrared absorption spectroscopy. *American Mineralogist*, 53, 777–800.

MANUSCRIPT RECEIVED JULY 29, 2005

MANUSCRIPT ACCEPTED DECEMBER 10, 2005

MANUSCRIPT HANDLED BY ANDREAS LUTTGE